PNAS RESEARCH ARTICLE | MICROBIOLOGY OPEN ACCESS

Identification of the *Bartonella* autotransporter CFA as a protective antigen and hypervariable target of neutralizing antibodies in mice

Lena K. Siewert[a,b,1], Aleksandr Korotaev[a], Jaroslaw Sedzicki[a], Katja Fromm[a], Daniel D. Pinschewer[b,2,3], and Christoph Dehio[a,2,3]

Edited by Rino Rappuoli, Toscana Life Sciences Foundation, Siena, Italy; received February 7, 2022; accepted April 27, 2022

The bacterial genus *Bartonella* comprises numerous emerging pathogens that cause a broad spectrum of disease manifestations in humans. The targets and mechanisms of the anti-*Bartonella* immune defense are ill-defined and bacterial immune evasion strategies remain elusive. We found that experimentally infected mice resolved *Bartonella* infection by mounting antibody responses that neutralized the bacteria, preventing their attachment to erythrocytes and suppressing bacteremia independent of complement or Fc receptors. *Bartonella*-neutralizing antibody responses were rapidly induced and depended on CD40 signaling but not on affinity maturation. We cloned neutralizing monoclonal antibodies (mAbs) and by mass spectrometry identified the bacterial autotransporter CFA (CAMP-like factor autotransporter) as a neutralizing antibody target. Vaccination against CFA suppressed *Bartonella* bacteremia, validating CFA as a protective antigen. We mapped *Bartonella*-neutralizing mAb binding to a domain in CFA that we found is hypervariable in both human and mouse pathogenic strains, indicating mutational antibody evasion at the *Bartonella* subspecies level. These insights into *Bartonella* immunity and immune evasion provide a conceptual framework for vaccine development, identifying important challenges in this endeavor.

Bartonella | neutralizing antibodies | red blood cell infection | autotransporter | immune evasion

Bartonella is a genus of gram-negative, facultative intracellular pathogens of mammals that are transmitted by blood-sucking arthropods (1–3). The genus comprises numerous emerging pathogens of clinical importance, most prominently *Bartonella bacilliformis*, *Bartonella quintana*, and *Bartonella henselae*, the causative agents of Carrion's disease, trench fever, and cat scratch disease, respectively. Infection can be life-threatening and the disease presents with a broad spectrum of symptoms depending on the pathogen and the immune status of the patient (4–6). Carrion's disease, for example, is vectored by sand flies and has affected the human population in South America since the days of the Inca (7). The resulting hemolytic fever ("Oroya fever") has a case-fatality rate of up to 90%. Climate change together with observations on the pathogen's vectoring by alternate sand fly species raises concerns that the disease may cause more widespread outbreaks in the coming decades (8). Still, prophylactic vaccines are unavailable.

Bartonellae are highly host-restricted pathogens and establish long-lasting intraerythrocytic bacteremia (1, 2, 9–11). This intracellular niche poses a formidable challenge to antibacterial immune defense and leaves important knowledge gaps with respect to the mechanisms of immune control. Studies on experimental *Bartonella* infection in mice showed that antibodies play an important role in the clearance of bacteremia (12), with some direct or indirect contribution by CD4 T cells (13). While the mechanisms accounting for antibody-mediated host defense remain understudied, it has long been speculated that antibodies may interfere with erythrocyte infection (12, 14, 15). Antisera raised against the flagellum or the invasion-associated locus B (IalB) protein of a selected *Bartonella* species impeded erythrocyte invasion by these bacteria in vitro (16, 17). It remains unknown, however, whether the same structures are targets of the protective antibody response in the natural infection context and whether neutralization represents a mechanistic correlate of anti-*Bartonella* antibody protection.

Neutralizing antibodies are best characterized in the context of viral infection, where they bind to surface structures on the infectious cell-free virion and prevent host cell receptor binding or membrane fusion (18). In the context of bacterial infections, antibody neutralization is more common for secreted toxins than for the infectious agents themselves (19). Antibody-mediated immunity against extracellular bacteria is most commonly accounted for by direct and/or complement-dependent opsonization. In addition, antibodies have been shown to inhibit the attachment of *Staphylococcus aureus*

Significance

Bartonella infections represent a significant burden to human health and are difficult to cure. Protective *Bartonella* vaccines are not available. Acquired immunity to *Bartonella* infection could provide a blueprint for vaccine design but remains incompletely defined. Moreover, bacterial immune evasion mechanisms have the potential to thwart vaccination efforts. Our study in a model of a natural *Bartonella*–host relationship revealed that antibody-mediated prevention of bacterial attachment to erythrocytes is sufficient for protection. We identified the bacterial surface determinant CFA (CAMP-like factor autotransporter) as a target of protective antibodies. While immunization with CFA protected against challenge with the homologous *Bartonella* isolate, extensive variability of CFA already at the strain level revealed bacterial immune evasion mechanisms with implications for *Bartonella* vaccine design.

This article is a PNAS Direct Submission.

[1]Present address: Experimental Neuroimmunology, Department of Biomedicine, University of Basel, 4056 Basel, Switzerland.

[2]D.D.P. and C.D. contributed equally to this work.

[3]To whom correspondence may be addressed. Email: christoph.dehio@unibas.ch or daniel.pinschewer@unibas.ch.

This article contains supporting information online at http://www.pnas.org/lookup/suppl/doi:10.1073/pnas.2202059119/-/DCSupplemental.

Published June 17, 2022.

to fibrinogen (20) and to inhibit the growth of *Borrelia* (21). In remarkable contrast to these extracellular pathogens, antibodies binding to the major outer-membrane protein of *Chlamydia trachomatis*, an obligate intracellular bacterium, have been demonstrated to prevent host cell attachment and antagonize bacterial internalization (22). Only limited evidence has, however, accumulated to support a similar concept for facultative intracellular bacteria such as *Mycobacterium tuberculosis* (23, 24), and a potential contribution of antibody-mediated neutralization to the resolution of natural infection remains elusive.

In this study, we explored the adaptive immune response to *Bartonella taylorii* in its natural host, the mouse. We establish neutralizing antibodies as a correlate of in vivo protection for this facultative intracellular bacterium and unravel the requirements for protective antibody formation. The identification of a protective *Bartonella* surface antigen in conjunction with extensive variability in its antibody-targeted domain offers insights into bacterial immune evasion with far-reaching implications for vaccine design and the *Bartonella*–host relationship in general.

Results

B Cell–Dependent Clearance of *Bartonella* Bacteremia and Passive Antibody Therapy. Studying the mouse model of *Bartonella* infection, we set out to characterize the adaptive immune response with special emphasis on the role B cells play in clearing bacteremia. To this end, we used *B. taylorii* IBS296, a strain naturally infecting mice (25). We first compared the course of bacteremia in wild-type (WT) C57BL/6 mice with gene-targeted mice lacking either only B cells (B cell ko [knockout]) or both B and T cells ($Rag1^{-/-}$) (Fig. 1*A*). Intradermal (i.d.) infection of WT mice was followed by a brief abacteremic window of 5 to 7 d. Bacterial titers in blood then rose to peak at 10 to 12 d post infection (d.p.i.) with $\sim 10^5$ colony-forming units (cfu) per milliliter of blood. The infection was cleared within 50 d.p.i. and relapses were never observed. These infection kinetics resembled earlier reports from small-rodent models of *Bartonella* infection (12, 26). In contrast, $Rag1^{-/-}$ or B cell ko mice showed lifelong persistent infection, reaching a plateau of up to 10^7 cfu per milliliter of blood (Fig. 1*A*). The lack of clearance in $Rag1^{-/-}$ and B cell ko mice confirmed earlier findings on the essential role of B cells in the clearance of *Bartonella grahamii* in mice (12). To directly assess the efficacy of antibodies in the *Bartonella* control, we performed transfer experiments with *B. taylorii*–reactive sera of WT mice (Fig. 1*B*). Immune serum transfer to bacteremic B cell ko mice on day 87 post infection caused bacteremia to subside (Fig. 1 *C* and *D*). Further, we established a prophylactic serum transfer protocol (Fig. 1*E*). WT mice obtained naïve or immune serum on day 3 post infection, thus in the abacteremic window. Recipients of naïve serum developed bacteremia, while the blood of mice given immune serum remained sterile (Fig. 1*F*). Thus, antibodies were effective in both clearing and preventing *Bartonella* bacteremia.

Immune Sera Interfere with *Bartonella* Adhesion to Erythrocytes While Complement and Fcγ-Receptors Are Dispensable for Bacterial Control in Mice. We aimed to test the long-standing but so far unproven hypothesis that antibodies interfere with *Bartonella* infection through neutralization defined as the prevention of erythrocyte infection (12, 14, 15). To quantify the protective capacity of immune sera, we modified an in vitro *Bartonella* erythrocyte infection assay previously published for *Bartonella birtlesii* (27). Murine erythrocytes were purified and incubated with green fluorescent protein (GFP)–expressing *B. taylorii* IBS296 (*SI Appendix*, Fig. S1*A*). Bacterial attachment to erythrocytes was quantified using flow cytometry. To assay for interference of protective antibodies with erythrocyte infection, bacteria were incubated with naïve or immune serum prior to the incubation with erythrocytes (Fig. 2*A*). Immune serum suppressed the amount of GFP+ erythrocytes in a concentration-dependent manner, whereas naïve serum had no observable effect (Fig. 2 *B* and *C*). Heat inactivation of complement in immune serum had no effect on the suppression of erythrocyte adhesion (*SI Appendix*, Fig. S1*B*). No significant bactericidal effect of the immune serum on *B. taylorii* IBS296 was observed by assaying for bacterial growth at the end of the erythrocyte infection assay (*SI Appendix*, Fig. S1*C*), indicating that the reduction of GFP+ erythrocytes by immune serum can unlikely be attributed to killing of the bacteria.

Previous studies on in vitro infection of erythrocytes showed that *Bartonella* remains extracellular at 24 h post infection (27). To investigate if our assay is limited to measuring the adhesion to the target cell, we performed confocal microscopy and observed *B. taylorii* IBS296 on the erythrocyte surface only but not in the cells' interior (Fig. 2*D*). We confirmed this finding using a gentamicin protection assay. Gentamicin does not enter eukaryotic cells and the treatment thus selectively kills extracellular bacteria, while intracellular bacteria survive. Indeed, *B. taylorii* IBS296 remained gentamicin-sensitive during incubation with erythrocytes. In comparison, erythrocytes obtained from infected mice contained mostly gentamicin-insensitive bacteria (Fig. 2*E* and *SI Appendix*, Fig. S1*E*), indicating a mostly intraerythrocytic localization as previously reported for other *Bartonella* species infecting rodents (15, 27).

We next aimed to assess the titer of neutralizing serum activity over the course of the infection and tested if the established erythrocyte adhesion inhibition (EAI) assay correlated with clearance. We infected WT mice and followed the animals' EAI titer over time (Fig. 2*F*). Between day 7 and day 14 post infection, the EAI titer rose sharply and was maintained throughout the bacteremic period and beyond, reaching titers of up to 1:1,024. Around the time when EAI serum activity became detectable, the level of bacteria stabilized, and over the subsequent weeks it steadily subsided. The appearance of EAI activity did not, however, result in immediate bacterial clearance. This was in line with the above in vitro findings, suggesting protective antibodies interfere with erythrocyte infection prior to bacterial internalization. Bacteria residing inside infected erythrocytes are, therefore, predicted to be protected. Given that the intraerythrocytic stage of *Bartonella* infection is nonhemolytic (15), a delayed washout of intraerythrocytic bacteremia is compatible with EAI as a main mechanism of anti-*Bartonella* antibody activity.

When following EAI titers after serum transfer into B cell ko mice (Fig. 1 *C* and *D* and *SI Appendix*, Fig. S1*D*), EAI titers reached detection limits within about 2 to 3 wk, and similar kinetics were observed when immune serum was transferred into uninfected B cell ko mice (*SI Appendix*, Fig. S1*D*), suggesting that EAI titers were not substantially masked by antibody binding to free bacteria in circulation. We conclude that antibodies clear the infection by interfering with bacterial attachment to erythrocytes and that the EAI assay can serve for the quantification of *Bartonella*-neutralizing antibody responses.

To test for a potential contribution of antibody Fc-dependent effector mechanisms in bacterial control, we infected mice lacking all α-chains of Fcγ-receptors as well as complement component C3

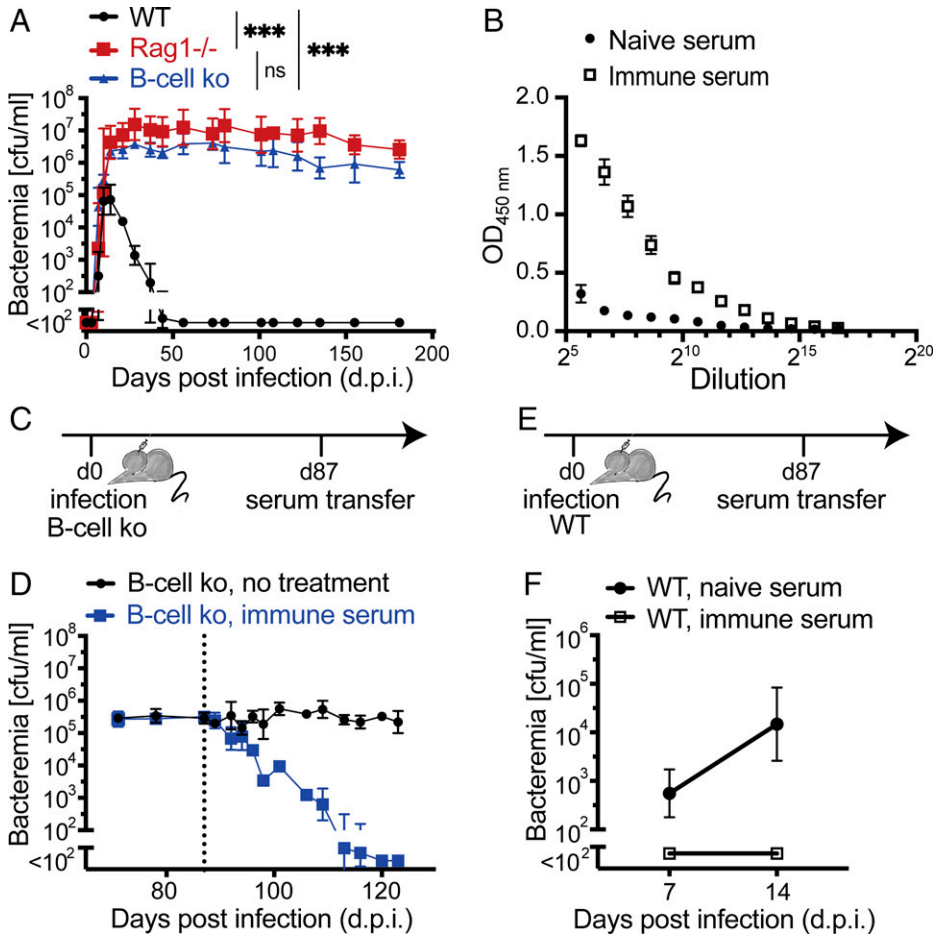

Fig. 1. B cell–dependent clearance of *Bartonella* bacteremia and passive antibody therapy. (*A*) Mice were infected i.d. with 10^7 cfu of *B. taylorii* IBS296, and bacteremia titers (cfu/mL blood) are shown for C57BL/6 WT, Rag1$^{-/-}$, and B cell ko mice up to 180 d.p.i. Symbols show the mean ± SD of at least four mice. (*B*) ELISAs were performed on plates coated with a *B. taylorii* IBS296 outer-membrane protein preparation. A pool of immune serum from 10 mice infected with *B. taylorii* for at least 45 d was compared with naïve serum. Symbols represent the mean ± SD of three technical replicates. (*C* and *E*) Schematic of the passive immunization experiments by serum transfer reported in the subsequent panels. *C* describes the experiment in *D*; *E* describes the experiment in *F*. (*D*) We infected B cell ko mice i.d. with 10^7 cfu of *B. taylorii* IBS296 and 87 d later, after establishment of persistent bacteremia, treated them intravenously with 100 μL of either naïve or immune serum raised against *B. taylorii* IBS296 as described in *B*. Bacteremia was followed over time; the dashed line indicates the time point of serum transfer (day 87 post infection). Symbols represent the mean ± SD of three mice. (*F*) WT mice were infected as for the experiment in *D* and were treated intraveneously with 100 μL of either naïve or *B. taylorii* IBS296 immune serum on day 3. Bacteremia was determined on day 14 and day 21 post infection. Symbols represent the mean ± SD of six mice. *A*, *B*, and *D* show representative data and *F* shows pooled data from two independent experiments. Statistical analysis was performed using two-way ANOVA, and *P* values are reported for comparisons evidencing statistically significant differences. ns, $P > 0.05$; ***$P \leq 0.001$.

(FcγRnull x C3$^{-/-}$). In this model, antibodies fail to activate complement or to mediate antibody-mediated cellular phagocytosis and related Fc-dependent effector functions. There was no difference in bacteremia kinetics between FcγRnull x C3$^{-/-}$ and WT mice (Fig. 2*G*), indicating that Fc-dependent effector mechanisms are dispensable and do not significantly contribute to *Bartonella* clearance. Accordingly, prophylactic transfer of immune serum protected FcγRnull x C3$^{-/-}$ mice analogous to the observations made in WT mice (Fig. 2 *H* and *I*, compare with Fig. 1 *E* and *F*).

***Bartonella* Clearance Depends on Antibody Specificity and CD40L, but Occurs Independent of Antibody Affinity Maturation and Isotype Class Switching.** To further assess the mechanistic requirements for a protective antibody response against *Bartonella*, we infected a range of gene-targeted mouse models and measured bacteremia and EAI antibody responses over time. In stark contrast to WT mice, B cell ko mice failed to mount an antibody response and became persistently infected, as expected (Fig. 3 *A* and *B*, compare with Fig. 1 *A* and *B*). B cells of mice deficient in activation-induced deaminase (AID$^{-/-}$ mice) cannot undergo affinity maturation or class-switch recombination, but AID$^{-/-}$ mice nevertheless mounted a largely normal EAI antibody response and controlled *Bartonella* similar to WT mice (Fig. 3*C*). sIgM$^{-/-}$ mice carry surface IgM on naïve B cells but are unable to secrete soluble immunoglobulin M (sIgM) and only secrete class-switched immunoglobulin isotypes. Nevertheless, sIgM$^{-/-}$ mice promptly produced *Bartonella*-specific antibodies and controlled the infection (Fig. 3*D*). These data indicated that either IgM or class-switched antibody responses alone sufficed to control *Bartonella* infection, and that the germline antibody repertoire was sufficient to effectively combat this pathogen. AID$^{-/-}$ x sIgM$^{-/-}$ double-deficient mice have B cells but owing to their combined deficiency are unable to secrete any immunoglobulins. Accordingly, these mice failed to mount antibacterial antibody responses and had unchecked bacteremia for the entire period of observation. While B cell ko mice are devoid of B cells as well as antibodies, these findings in AID$^{-/-}$ x sIgM$^{-/-}$ mice documented that it was the antibody production rather than any other role of B cells in the immune response that controls *Bartonella* infection (Fig. 3*E*). Enzyme-linked immunosorbent assays (ELISAs) were conducted and confirmed that WT mice

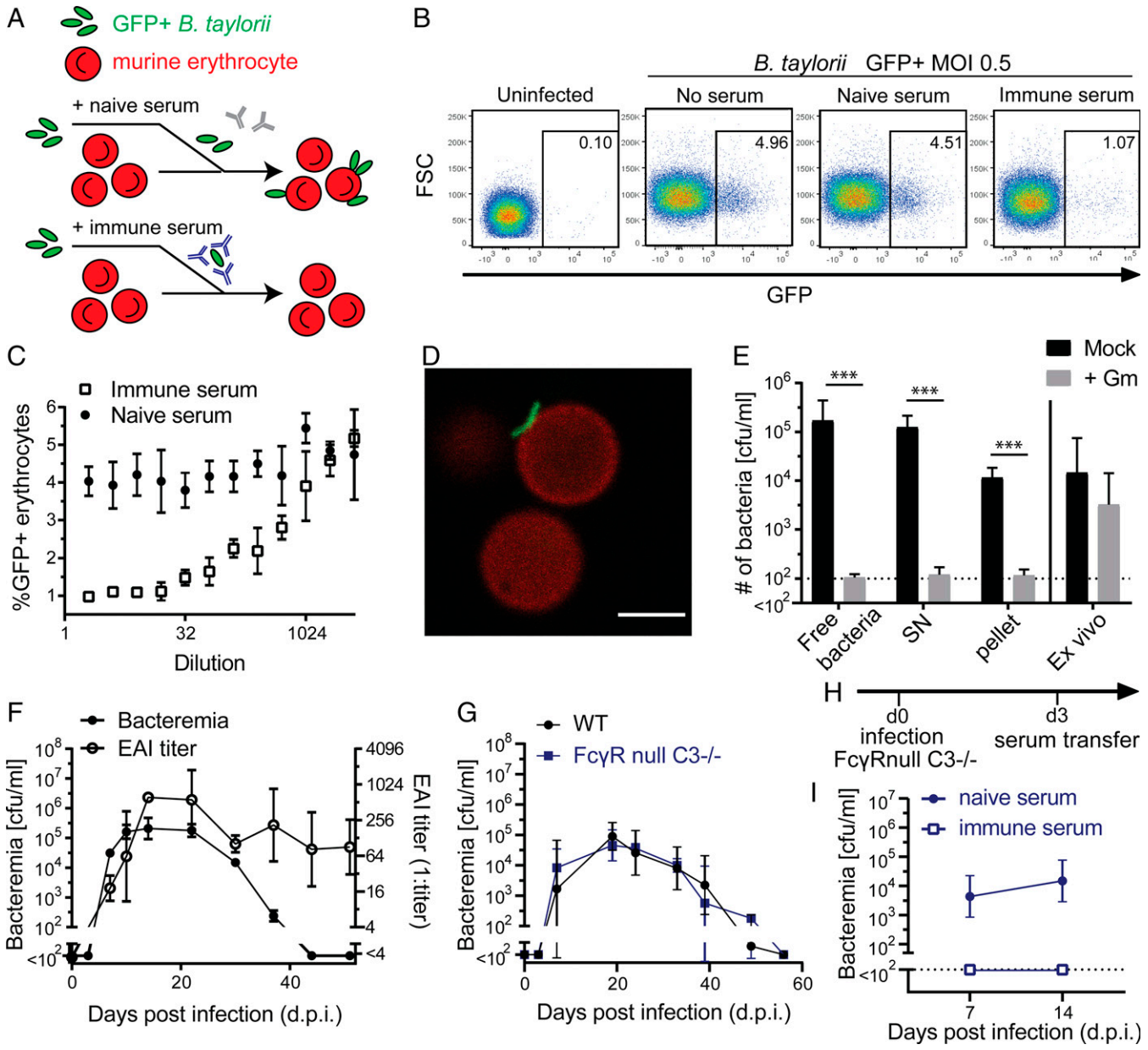

Fig. 2. Immune sera interfere with *Bartonella* adhesion to erythrocytes while complement and Fcγ-receptors are dispensable for bacterial control in mice. (*A*) Schematic of the EAI assay. (*B*) Exemplary flow cytometry pseudocolor plots of erythrocytes from the EAI assay: control erythrocytes without addition of *Bartonella* (uninfected) or erythrocytes incubated with GFP-expressing bacteria that have been mock-incubated without serum (no serum) or have been incubated with either naïve (naïve serum) or *Bartonella*-immune serum (immune serum). FSC = forward scatter. (*C*) The above EAI assay was conducted using serially diluted serum. The attachment rate in the presence of serially diluted either naïve or immune serum is reported as % GFP+ erythrocytes. (*D*) Confocal images of murine erythrocytes (stained with anti-Ter119 antibody; red) and incubated with GFP-expressing *B. taylorii* IBS296 (MOI 0.5; green). (Scale bar, 3 μm.) (*E*) Gentamicin (Gm) protection assays were performed with *B. taylorii* prepared and obtained as follows: Bacteria were either used directly from the plate (free bacteria) or incubated with erythrocytes (MOI 0.5) in vitro for 24 h followed by centrifugation to pellet erythrocytes. The resulting supernatant (SN) and pellet were assayed individually. For comparison, erythrocytes were prepared from mice infected with 10^7 cfu of *B. taylorii* IBS296 14 d before (ex vivo). (*F*) Bacteremia and EAI antibody titers were monitored longitudinally in WT C57BL/6 mice infected i.d. with 10^7 cfu of *B. taylorii* IBS296. (*G*) Bacteremia titers shown for WT compared with FcγRnull x $C3^{-/-}$ mice. (*H*) Schematic of the serum transfer passive immunization experiments in *I*. (*I*) We infected FcγRnull x $C3^{-/-}$ mice i.d. with 10^7 cfu of *B. taylorii* IBS296 and 3 d later treated them with 100 μL of either *B. taylorii* IBS296–immune (>45 d) or naïve serum. Bacteremia was determined on day 7 and day 14 post infection. (*C* and *E*) Symbols show mean and SD of technical replicates; representative results are shown from one out of three independent experiments. (*D*) One representative image from 50,000 erythrocytes analyzed by fluorescence microscopy. Symbols in *F* represent the mean of three mice and in *G* the mean of four mice per group; both are representative of two independent experiments. Pooled data from two independent experiments with a total of six mice are shown in *I*. Error bars indicate SD. Statistical analysis in *E* was performed using unpaired Student's *t* test and statistically significant differences are indicated as ***$P \leq 0.001$. See also *SI Appendix*, Fig. S1.

produced *Bartonella*-specific IgM and IgG and $AID^{-/-}$ mice produced only IgM, whereas $sIgM^{-/-}$ mice were devoid of anti-*Bartonella* IgM but produced class-switched antibodies (*SI Appendix*, Fig. S2*A*). To specifically address a potential role of complement in IgM-mediated bacterial clearance, we tested infection control and antibody responses in $AID^{-/-}$ x $C3^{-/-}$ double-deficient animals but did not find a clear difference in bacterial clearance kinetics or EAI antibody responses (*SI Appendix*, Fig. S2*B*).

To test whether antibody specificity was important for anti-*Bartonella* defense, we used T11μMT mice, which have an almost monoclonal B cell repertoire directed against a

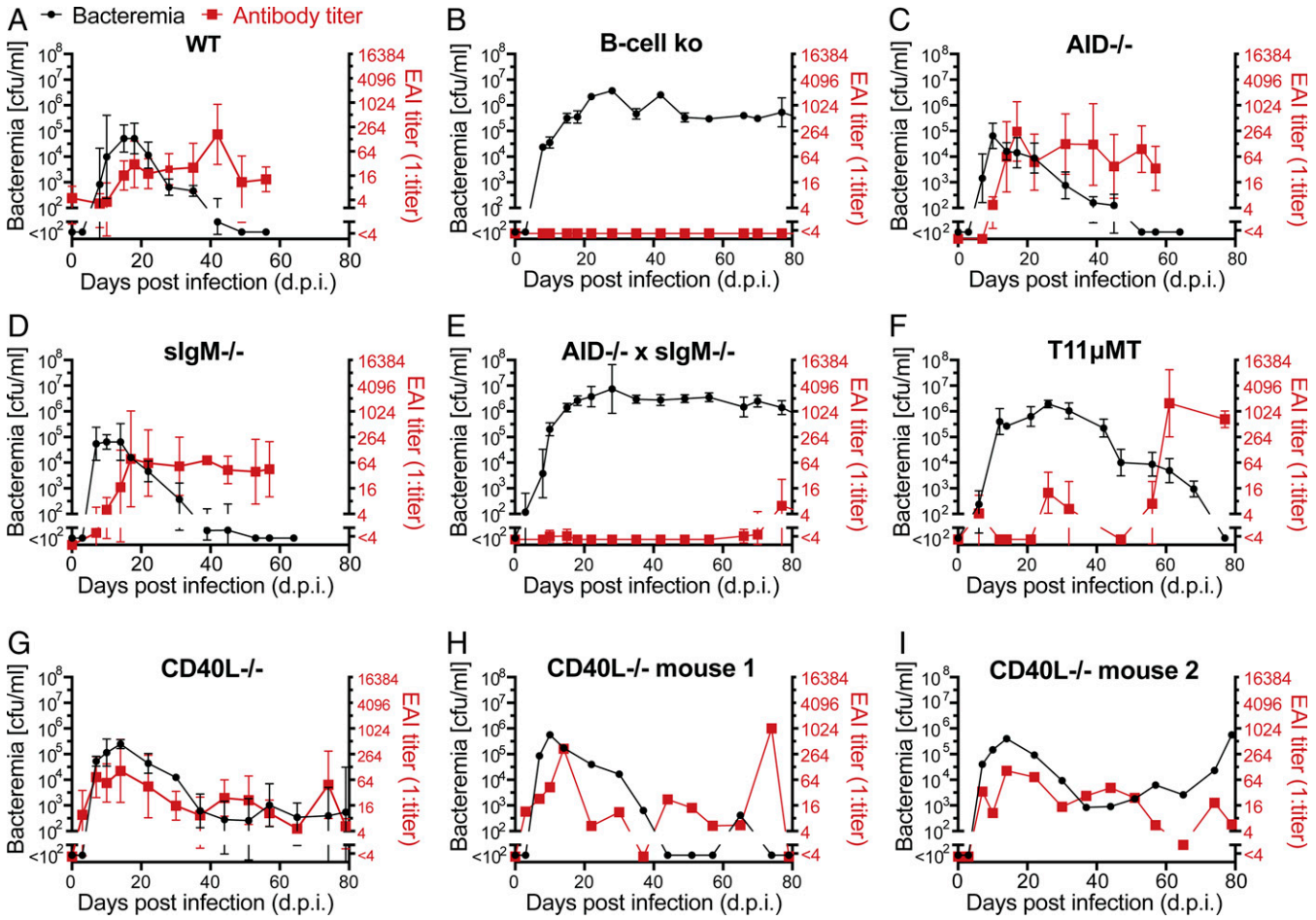

Fig. 3. *Bartonella* clearance depends on antibody specificity and CD40L, but occurs independent of antibody affinity maturation and isotype class switching. (*A*–*G*) We infected groups of mice of the indicated genotypes with 10^7 cfu of *B. taylorii* IBS296 and followed bacteremia as well as EAI titers over time. (*H* and *I*) These parameters are for two individual mice of the experiment shown in *G*. Data of additional individual CD40L$^{-/-}$ mice are displayed in *SI Appendix*, Fig. S2. Representative data from two independent experiments are reported as mean ± SD. Symbols in *A* and *D*–*F* show the mean of four mice and symbols in *B* report the mean of three mice; symbols in *C* and *G* display the mean of five mice per group.

Bartonella-unrelated viral antigen (28). Accordingly, the *Bartonella* EAI antibody response of T11µMT was substantially delayed. Bacteremia persisted approximately twice as long as in WT mice and only subsided with the advent of a delayed albeit eventually robust antibody response (Fig. 3*F*).

CD4 T cells have been reported to contribute to *Bartonella* clearance (13) and T help generally requires T cell–B cell interactions involving CD40L–CD40 signaling. In the first 30 to 40 d post *Bartonella* infection, CD40L$^{-/-}$ mice controlled bacteremia and mounted antibody responses similar to WT mice. At later time points, however, CD40L$^{-/-}$ mice exhibited intermittent drops in antibody titers, which varied between individual mice, and the animals failed to completely eliminate *Bartonella* or evidenced rebound bacteremia after a period of transient bacterial control (Fig. 3 *G*–*I* and *SI Appendix*, Fig. S2 *C*–*E*). Unsustained antibody responses and incomplete pathogen control by CD40L$^{-/-}$ mice mimicked these animals' behavior in other infection models (29, 30) and indicated CD40L-dependent helper functions were essential for sustained antibody responses and complete *Bartonella* control.

Cloning and Characterization of Protective Monoclonal Antibodies against *B. taylorii*. In light of this key role of the antibody response in the clearance of *Bartonella* infection, we set out to identify the molecular target(s) of neutralizing antibodies. We generated hybridomas from BALB/c mice immunized with *B. taylorii* IBS296 and identified two promising monoclonal antibodies (mAbs) that interfered with *Bartonella* adhesion to erythrocytes in vitro (LS4G2 and LS5G11; Fig. 4 *A* and *B*). The LS4G2 hybridoma was of the IgG3 and LS5G11 of the IgG2a isotype. The two antibodies originated from different germline V(D)J elements, and thus were clonally unrelated. To improve comparability, both antibodies were recombinantly expressed in the IgG2a format for the subsequent experiments. LS4G2 and LS5G11 bound to the bacterial surface (Fig. 4 *C* and *D*) yet lacked a detectable bactericidal effect (*SI Appendix*, Fig. S3*A*). Strikingly, both antibodies were highly specific for the *B. taylorii* IBS296 strain used for immunization and failed to bind another *B. taylorii* isolate (strain M1) or other, closely related *Bartonella* species (*SI Appendix*, Fig. S3*B*). Since both antibodies were selected for their in vitro activity, we wanted to test if they are also protective in vivo. To this end, we infected mice with *B. taylorii* IBS296 and 3 d later treated them with either LS4G2, LS5G11, or an isotype control antibody. The blood of recipients of LS4G2 and LS5G11 remained sterile, while those given an isotype control antibody became bacteremic (Fig. 4 *E* and *F*). These findings indicated that the EAI assay identified antibodies that exhibited in vivo protective capacity. Analogous results for LS4G2 passive immunization were obtained in FcγRnull x C3$^{-/-}$ mice (Fig. 4 *G* and *H*), further supporting the conclusion that LS4G2 protected by neutralizing *Bartonella* independent of classical complement- or Fc-mediated effector functions.

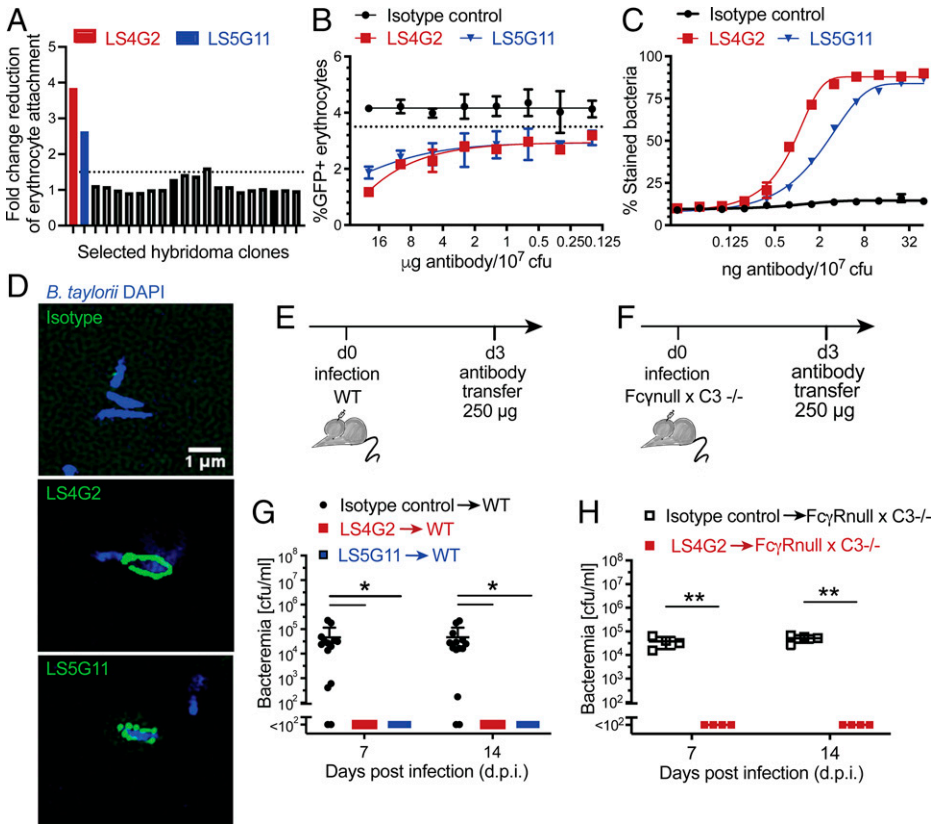

Fig. 4. Cloning and characterization of protective mAbs against *B. taylorii* IBS296. (*A*) Supernatants collected from 20 individual hybridoma clones in our screen were analyzed using EAI assays. The potency of each clone is expressed as fold-change reduction of erythrocyte attachment when compared with mock (medium only). The two most potent clones (LS4G2 and LS5G11) are highlighted in red and blue, respectively. (*B*) The EAI potency of purified LS4G2 (red) and LS5G11 (blue) in side-by-side comparison with an isotype control antibody. (*C*) *B. taylorii* IBS296 surface staining by LS4G2 (red), LS5G11 (blue), and an isotype control antibody was quantified by flow cytometry. (*D*) Surface labeling of *B. taylorii* IBS296 (DAPI; blue) upon incubation with LS4G2, LS5G11, or an isotype control antibody (all in green) was visualized by structured illumination microscopy. (*E–H*) Schematic of passive immunization antibody transfer experiments conducted in *F* (schematic in *E*) and *H* (schematic in *G*): WT (*F*) and FcγR null x $C3^{-/-}$ mice (*H*) were infected i.d. with 10^7 cfu of *B. taylorii* IBS296 and 3 d later were treated with 250 µg of the indicated antibodies intravenously. Bacteremia was determined on day 7 and on day 14 post infection. (*B–D*) One representative dataset from two independent experiments is shown. Each experiment was performed in technical triplicates. (*F*) Pooled data from three independent experiments are reported. Symbols in *F* and *H* represent individual mice ($n = 10$ per group in *F*; $n = 4$ per group in *H*). Statistical analysis was performed by unpaired Student's *t* tests; $^*P \leq 0.05$, $^{**}P \leq 0.01$. Error bars show SD. See *SI Appendix*, Fig. S3 for related data.

The *B. taylorii* Autotransporter CFA Is a Target of Protective Antibodies. To identify the bacterial targets of the two protective mAbs, we performed immunoprecipitations from the solubilized outer-membrane fraction of *B. taylorii* IBS296 followed by mass spectrometry. Surprisingly, both antibodies pulled down the same protein: OPB34894.1 (Fig. 5 *A* and *B*). The ortholog in *B. henselae* was previously identified as an autotransporter with a putative cohemolysin activity and has been termed a CAMP-like factor autotransporter (CFA) (31). Autotransporter proteins constitute a large family of virulence factors secreted by gram-negative bacteria via the type V secretion mechanism. They are characterized by an extracellular passenger domain at the N terminus that often remains anchored in the outer membrane via a C-terminal β-barrel (32). Deletion of the *cfa* locus in *B. taylorii* IBS296 resulted in complete loss of binding by LS4G2 and LS5G11, a phenotype which could be rescued by the expression of the protein from a plasmid (Fig. 5*C*). Finally, the expression of CFA of *B. taylorii* IBS296 (CFA_{Btay}) in other *Bartonella* species, which in their native form failed to react with our mAbs, resulted in surface staining (*SI Appendix*, Fig. S3 *B–D*). Altogether, these observations validated CFA as the molecular target of the protective antibodies LS4G2 and LS5G11.

CFA has been shown essential for *Bartonella tribocorum* bacteremia in rats (33) and *B. birtlesii* bacteremia in mice (27). We extended these findings to *B. taylorii* IBS296. Since tools for chromosomal in vivo complementation of *B. taylorii* mutants remain unavailable, we infected mice either with three independent deletion mutant clones or with the corresponding isogenic revertant WT variant, which underwent the exact same genetic manipulation procedure and are identical except for the presence or absence of the *cfa* locus. Indeed, the blood of the animals infected with the Δ*cfa* locus mutant remained sterile, while revertant WT bacteria caused normal bacteremia (Fig. 5*D*).

B. tribocorum naturally infects rats but does not cause robust bacteremia in mice (15). Here, we used it as a prototypic live vaccine vector to test whether CFA is a protective antigen in *B. taylorii* IBS296. We vaccinated mice with an isogenic *B. tribocorum* strain, which we engineered to ectopically express CFA_{Btay}, whereas control animals were administered WT *B. tribocorum*. Six weeks post immunization, we challenged both groups of mice with *B. taylorii* IBS296. All control mice immunized with WT *B. tribocorum* developed *B. taylorii* IBS296 bacteremia. In contrast, one-third of the mice vaccinated with *B. tribocorum* expressing CFA_{Btay} remained abacteremic (Fig. 5*E*). The other two-thirds of vaccinated mice, albeit developing bacteremia, exhibited a significantly reduced peak bacterial burden and a shortened duration of bacteremia (Fig. 5 *F–H*). Importantly, mice immunized with *B. tribocorum* expressing CFA_{Btay} developed EAI antibodies within the first 7 d after challenge, whereas the control group only did so by day 14 (Fig. 5*I*). Taken together, these experiments identified the autotransporter CFA as a protective antibody target and candidate vaccine antigen in *Bartonella*.

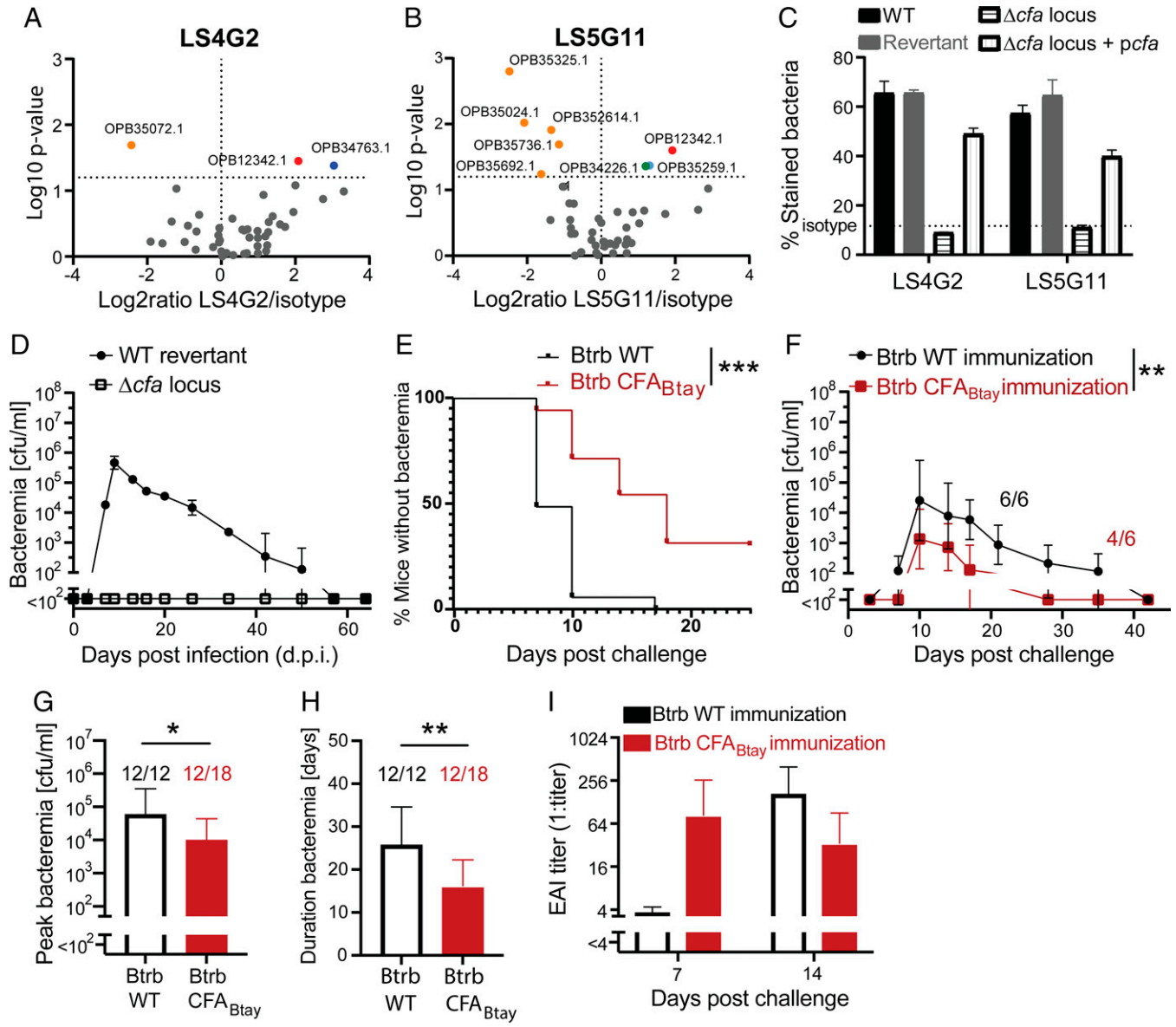

Fig. 5. *B. taylorii* autotransporter CFA is a target of protective antibodies. (*A* and *B*) Volcano plots of proteins identified by mass spectrometry after pull-down with either LS4G2 (*A*) or LS5G11 (*B*). OPB12342 denominates the gene product of *cfa*. The second LS4G2 hit OPB34763.1 could not be confirmed in a repeat experiment and hence was not pursued further. (*C*) To validate CFA as a molecular target of the LS4G2 and LS5G11 mAbs, we stained the following versions of *B. taylorii* IBS296 and determined surface-bound antibody by flow cytometry: 1) the parental WT bacterium, 2) the *cfa* locus ko mutant (Δ*cfa* locus), 3) the corresponding WT "revertant" strain, and 4) the *cfa* locus ko strain complemented by the expression of *cfa* from plasmid (Δ*cfa* locus + p*cfa*). Note that the WT revertant and the Δ*cfa* locus ko mutant are isogenic strains, which are progeny of the same bacterial mutagenesis intermediate but represent the result of independent recombination events in different homology regions, both leading to the deletion of a transiently integrated mutagenesis plasmid. Symbols represent the mean ± SD of three technical replicates. (*D*) We infected WT C57BL/6 mice i.d. with 10^7 cfu of either WT revertant or the Δ*cfa* locus deletion mutant of *B. taylorii* IBS296 and monitored bacteremia over time. Symbols represent three mice per group, each infected with an independent clone of deletion mutant or revertant. (*E*–*I*) We immunized C57BL/6 WT mice i.d. either with 10^7 cfu of WT *B. tribocorum* (Btrb WT) or with the same dose of an isogenic strain expressing CFA of *B. taylorii* IBS296 (Btrb CFA_{Btay}). Six weeks later, both groups of mice were challenged with *B. taylorii* IBS296. (*E*) The percentage of abacteremic mice as a function of time. Combined data from three experiments with three to six mice per group each. (*F*) Bacterial loads in blood are selectively reported only for bacteremic animals (6/6 Btrb WT-immunized mice; 4/6 Btrb CFA_{Btay}-immunized mice) from one out of three experiments. (*G* and *H*) Peak bacteremia (*G*) and duration of bacteremia (*H*) for bacteremic animals (12/12 Btrb WT-immunized mice; 12/18 Btrb CFA_{Btay}-immunized mice). Combined data from three independent experiments. (*I*) EAI titers of the animals in *F* were determined on day 7 and day 14 after *B. taylorii* challenge. (*A*–*D*) Representative data from two independent experiments are shown. For statistical analysis, we used the log-rank test (*E*), two-way ANOVA (*F*), and unpaired Student's *t* test (*G* and *H*); $*P \le 0.05$, $**P \le 0.01$, $***P \le 0.001$. Data in *C*, *D*, *F*, and *I* are reported as mean ± SD; mean ± SEM is shown in *F*.

High Variation of CFA on the Subspecies Level Suggests Immune Evasion from Antibody Selection Pressure. We next performed a comparative genomics analysis among the Bartonellae to learn more about the structure of the *cfa* locus as well as about the level of conservation and sequence variation in CFA. We found that the *cfa* locus is present in all Eubartonellae (*SI Appendix*, Fig. S3*E*). The locus is composed of the *cfa* gene, immediately followed by a variable number of downstream genes or pseudogenes with homology to *cfa*, suggesting that those represent remnants of gene duplication or recombination events. The *cfa* locus is flanked by synteny blocks consisting of highly conserved genes responsible for iron uptake (*fatBCD*, located upstream) and accountable for creatin and cobalamin metabolism (BH12990 to BH12970, located downstream), respectively (Fig. 6*A*).

Protein-folding predictions using AlphaFold (35) indicated that the passenger domain of CFA is composed of

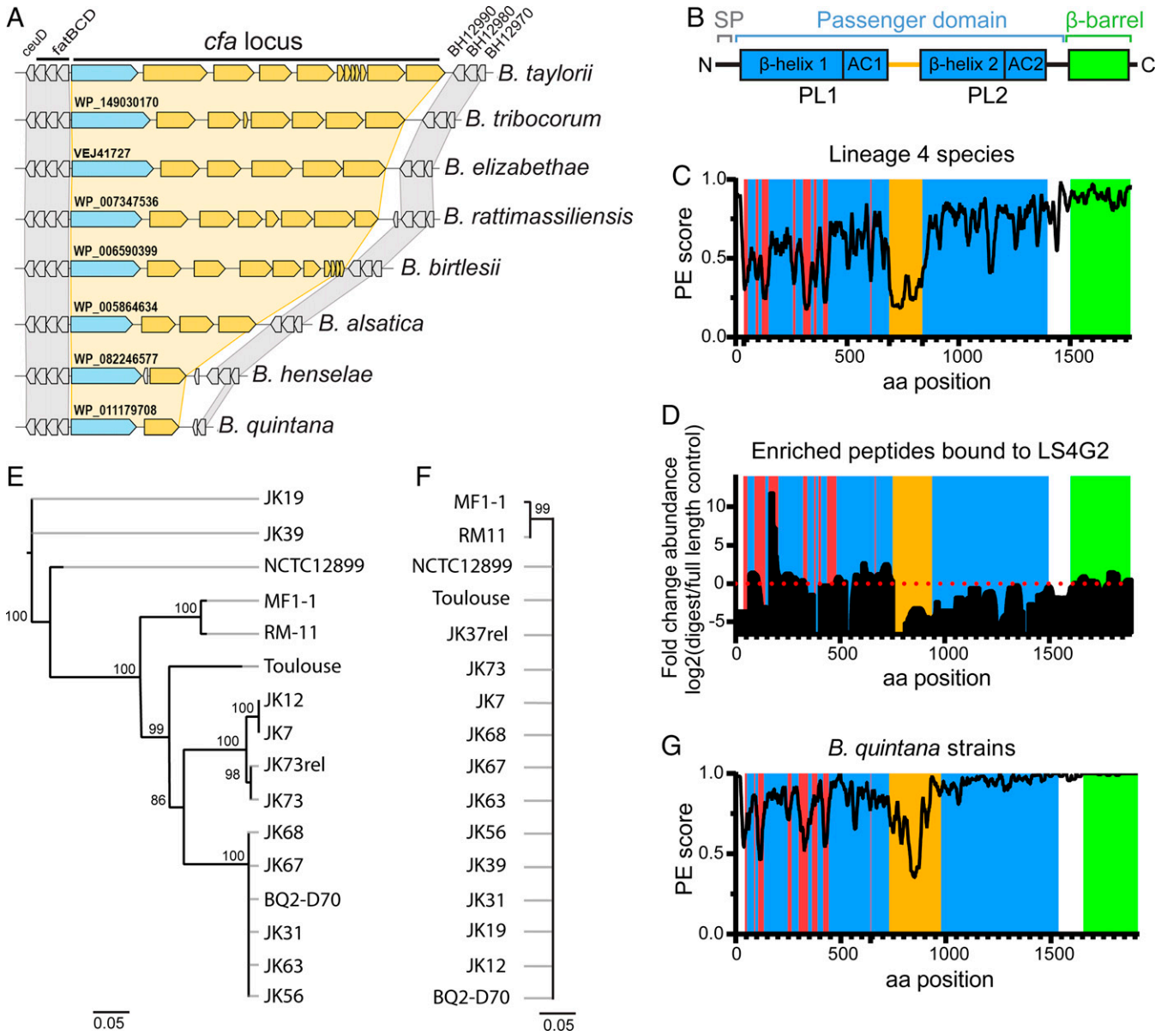

Fig. 6. High variation of CFA on the *Bartonella* subspecies level suggests immune evasion from antibody selection pressure. (*A*) Gene synteny analysis of the *cfa* locus and flanking regions in the indicated *Bartonella* species. Flanking housekeeping genes are shown in gray, the *cfa* locus is shown in blue with the corresponding gene annotation, and further putative autotransporter genes/pseudogenes are shown in yellow. (*B*) Domain organization of CFA of *B. taylorii* IBS296. SP (signal peptide; gray), the surface-located passenger domain with two β-helices (blue), pertactin-like domains (PL), and corresponding autochaperones (AC) predicted to form two stalks, separated by a linker (orange) and the C-terminal β-barrel (green). (*C* and *G*) Conservation scores of amino acid (aa) sequences along alignments of CFA homologs for (*C*) representative species of *Bartonella* lineage 4 or (*G*) closely related strains of *B. quintana*. The PE (property entropy) score is a metric based on Shannon entropy (34). The coloring scheme is based on colors used to illustrate CFA domain organization in *B*, except for the red color indicating hypervariable regions. (*D*) Analysis of putative LS4G2-binding regions in CFA of *B. taylorii* IBS296. After LS4G2 immunoprecipitation of CFA from bacterial lysates, a partial digest with proteinase K was performed and the eluted peptides were compared with full-length eluted (undigested) protein by mass spectrometry. Data are represented as fold-change difference between the above two conditions. The domain architecture is depicted including regions of high variability between *B. taylorii* strains IBS296 and M1 (red). Representative data from two independent experiments are reported, each performed in biological triplicates. (*E* and *F*) Phylogeny analyses of the indicated *B. quintana* strains were generated for the genes encoding either *cfa* (*E*) or *virB5* (*F*). Values above nodes show bootstrap support (>75%). Scale bars indicate the number of substitutions per site. See *SI Appendix*, Figs. S4 and S5 for further details.

two β-helices separated by a disordered linker (Fig. 6*B*). Each β-helix contains a predicted pertactin-like (PL1, PL2) fold including a C-terminal autochaperone (AC1, AC2) (36).

Comparative sequence analysis of CFA across lineage 4 species indicated that the level of sequence conservation of the passenger domain is inhomogeneous. We found that the N-terminal stalk, which is likely the distal part of CFA exposed on the bacterial surface, contains eight variation hotspots (V1 to V8; red in Fig. 6*C* and *SI Appendix*, Figs. S4 and S5*A*) and thereby overall is less conserved than the C-terminal stalk located closer to the membrane anchor. Structure prediction indicated that these variable regions overlap with parts of the polypeptide chain that do not form structural elements of the β-helix fold but rather decorate its surface, likely projecting outward (*SI Appendix*, Fig. S5 *B* and *C*).

We next aimed at mapping the LS4G2 epitope on CFA. We performed immunoprecipitation of CFA followed by limited proteolysis with proteinase K and compared the eluted peptides with the undigested full-length protein by mass spectrometry

(Fig. 6*D*). This approach revealed a supposed LS4G2-binding region in the distal (N-terminal) half of the passenger domain, located around amino acid positions 170 to 190. This region overlaps with one of the variation hotspots (V3) (*SI Appendix*, Figs. S4*A* and S5*C*), which exhibits substantial sequence differences between *B. taylorii* isolates IBS296 and the M1 isolate that is not bound by LS4G2 (*SI Appendix*, Figs. S3*B*, S4*A*, and S5*C*) and which we identified in our comparative analysis of lineage 4 species (Fig. 6*C*, highlighted in red; *SI Appendix*, Fig. S4*B*). This finding suggested that variation in this antigenic region of CFA may facilitate immune escape. We aimed to generalize and extend these findings to the human pathogen *B. quintana* (Fig. 6 *E*–*G* and *SI Appendix*, Fig. S4*C*), for which a large number of closely related isolates were collected from patients in San Francisco during the AIDS epidemic (*SI Appendix*, Table S1). We found that the pattern of variability hotspots on the subspecies level was similar to that observed at the species level in lineage 4 (Fig. 6*G*, compare with Fig. 6*C*; *SI Appendix*, Fig. S4 *B* and *C*). Strikingly, the variability of CFA sequences was significantly higher than the one in VirB5, an important virulence factor of *Bartonella*, which remained almost unchanged at the strain level (Fig. 6 *E* and *F*). Collectively, our findings document high variability in the surface-exposed regions of CFA and demonstrate these same regions might be the targets of neutralizing antibodies. Taken together, this pinpoints to antibody selection pressure accelerating the evolution of this protein domain, representing a supposed hotspot of mutational immune escape.

Discussion

This study demonstrates that neutralizing antibody responses represent a key pillar of effective immune defense against *Bartonella*, a facultative intracellular bacterium. We decipher not only the kinetics of protective antibody responses and the immunological processes underlying their formation but also their mechanism of action and the nature of their molecular targets. Thereby, the present work redefines our general understanding of *Bartonella*–host interactions, sharpens concepts of the germ's habitat in mammalian hosts, and offers prospects for vaccine design.

We show that CFA is a key molecular target of protective antibodies, although perhaps not the only one. Its sequence hypervariability in antibody binding sites suggests that *Bartonella* is under antibody selection pressure in the wild and evades it at the subspecies level of individual strains. We propose that CFA hypervariability may facilitate multiple sequential or even timewise overlapping infection episodes of the same mammalian host by closely related *Bartonella* strains. Besides enlargement of the bacterial habitat in time and host space, superinfection as a consequence of antibody evasion should create opportunities for gene transfer between different *Bartonella* strains as discussed below and thus is expected to expedite the evolution of the species.

CFA is present in all Eubartonellae, yet its variability extending to the strain level indicates that immune escape rather than host adaptation drives its evolution. The genomic organization of the *cfa* locus, with the *cfa* gene followed by multiple homologous genes, gene fragments, and/or pseudogenes, suggests that recombination rather than the accumulation of single–base pair changes is driving this process. The lack of recurrence of bacteremia in the experimental model suggests further that immune evasion depends on horizontal gene transfer between a larger pool of variant sequences that have evolved in closely related strains coexisting in the wild. As such, the described *Bartonella* gene transfer agent, which has been shown to mediate high-frequency exchange of genetic information between different Bartonellae (37, 38), might be mediating this horizontal gene transfer and is likely to contribute to the antigenic variation of CFA with resulting immune escape.

For vaccine development, the hypervariability of a key protective antibody target has important conceptual implications. CFA hypervariability resembles the immune evasion strategy of microbes such as the malaria parasite *Plasmodium falciparum* with its vast antigenic variation in adhesion molecules (39, 40), the extensive diversity in streptococcal cell-wall polysaccharides (41), or gonococcal pilus variants (42) but also the far over 100 known rhinovirus capsid serotypes (43). Unlike for influenza A virus, these pathogens do not depend on their serial replacement over time by new antigenic variants. On the contrary, a large number of variants cocirculate in host communities. We report that immunization with vectored CFA matching the *Bartonella* challenge isolate reduces peak bacterial burden and shortens the duration of bacteremia. However, only one-third of the animals remained abacteremic upon challenge, indicating that CFA-specific immunity alone does not consistently afford complete protection. A vaccine for human use would ideally cover all important pathogenic species or should at least encompass most strains of a given high-incidence species such as *B. henselae* or *B. quintana* that are responsible for most human infections worldwide. Notwithstanding its hypervariability, CFA may represent a promising candidate for inclusion in a multivalent vaccine. Antigen design could focus antibody responses on conserved regions and epitopes of CFA, resembling ongoing efforts in epitope-focused vaccine design for HIV, hepatitis C virus, and influenza A virus (44). If broadly subspecies–cross-protective antibodies can be induced by heterologous reinfection, their footprint on CFA will help in identifying conserved protective epitopes.

It remains to be investigated whether *Bartonella* carries other protective targets (16, 17), which may be invariant or less variable than CFA and thus more easily exploitable for vaccine design. Both protective antibodies identified in our study target CFA but, in light of the limited number of antibodies screened, it remains entirely possible that the protective antibody response to *Bartonella* infection comprises additional antigenic specificities. Besides the numeric limitations of our screen, the screening method relied on bacteria grown on agar plates, such that alternative antibody targets would have escaped detection if their expression was restricted to infection conditions. Similarly, antibodies interfering with steps of the bacterial life cycle other than erythrocyte adhesion would have gone undetected in our EAI assay.

Taken together, this study provides clear evidence for an evolutionary hide and seek between *Bartonella* and its natural rodent host. These findings advance our understanding of the *Bartonella*–host relationship, delineate key challenges in vaccine design, and help in devising strategies for how to meet them in order to combat this emerging human pathogen.

Materials and Methods

More detailed protocols can be found in *SI Appendix*.

Bacterial Strains and Growth Conditions. *Escherichia coli* and *Bartonella* strains were cultured as previously described (45). See *SI Appendix* for further details. All bacterial strains and plasmids used in this study are listed in *SI Appendix*, Tables S1 and S2.

Constructions of Strains and Plasmids. A detailed description for the construction of each plasmid, including oligonucleotide primers and synthesized gene fragments, is described in *SI Appendix* and listed in *SI Appendix*, Tables S2–S4.

Animal Experimentation. All experimental work with animals was approved by the Veterinary Office of the Canton Basel City (license no. 1741). Animals were infected or immunized i.d. with 10^7 cfu of bacteria in phosphate-buffered saline. Used mouse lines and detailed experimental procedures for plating of blood samples and serum generation are presented in *SI Appendix*.

Erythrocyte Infection and EAI Assay. See *SI Appendix* for a detailed experimental procedure for erythrocyte infection and the EAI assay. In brief, a serial dilution of sera or antibodies was incubated with bacteria for 1 h, before the addition of mouse erythrocytes (multiplicity of infection [MOI] 0.5). After 24 h, samples were fixed and analyzed by flow cytometry.

Gentamicin Protection Assay. Blood from infected animals or in vitro infected erythrocytes was incubated for 2 h in 40 μg/mL gentamicin. Cells were washed, lysed, and plated in serial dilutions on blood agar plates. For further details, see *SI Appendix*.

Hybridoma Production and Handling. For hybridoma production, the DiSH Kit (Enzo Life Sciences, ENZ-71001-0001) was used according to the manufacturer's protocol. For further details, see *SI Appendix*.

Purification of Monoclonal Antibodies. The sequences, cloning, and expression strategies of the LS4G2 and LS5G11 V_L and V_H regions are given in *SI Appendix, Materials and Methods* and Table S4.

Mass Spectrometry. Detailed instrument settings and data analysis can be found in *SI Appendix*. The mass spectrometry proteomics data have been deposited in the ProteomeXchange Consortium via the PRIDE (46) partner repository with the dataset identifier PXD028783 and 10.6019/PXD028783.

DNA Extraction and Sequencing. The genome sequences of *B. taylorii* IBS296 and M1 have been deposited under accession nos. CP083444 and CP083693, respectively. Detailed information on genome sequencing, assembly, and annotation can be found in *SI Appendix*.

Bioinformatic Analysis. A detailed description of the bioinformatic analysis including set parameters can be found in *SI Appendix*; the database from annotated genome sequences of *Bartonella* species can be found in *SI Appendix*, Table S5.

Data Analysis. Unless stated differently, statistical analysis of the obtained data was performed using GraphPad Prism software and the statistical tests as indicated. *P* values are depicted as follows: ns (not significant), $P > 0.05$; $*P \leq 0.05$, $**P \leq 0.01$, $***P \leq 0.001$. For further details on the liquid chromatography–mass spectrometry analysis, see *SI Appendix*.

Data Availability. The proteomics data (pull-down assays) and genome sequence data reported in this article have been deposited as follows: proteomics:ProteomeXchange Consortium via the PRIDE partner repository, dataset identifier PXD028783 and 10.6019/PXD028783; genomes: NCBI (national center for biotechnology information), *B. taylorii* IBS296 accession no. CP083444 and *B. taylorii* M1 accession no. CP083693.

All study data are included in the article and/or *SI Appendix*.

ACKNOWLEDGMENTS. We thank Stefan Bienert, Alexander Harms, Marianna Florova, Richard Neher, and Alexander Wagner for their valuable input into planning the experimental design and approaches. This work was supported by Swiss National Science Foundation (SNSF; www.snf.ch) Grants 310030B_201273 (to C.D.) and 310030_173132 to (D.D.P.), the National Centre of Competence in Research AntiResist funded by SNSF Grant 51NF40_180541 (to C.D.), as well as by European Research Council Grant 310962 (to D.D.P.).

Author affiliations: [a]Biozentrum, University of Basel, 4056 Basel, Switzerland; and [b]Division of Experimental Virology, Department of Biomedicine, University of Basel, 4009 Basel, Switzerland

Preprint: L. K. Siewert et al., "The *Bartonella* autotransporter CFA is a protective antigen and hypervariable target of neutralizing antibodies blocking erythrocyte infection" (2021). bioRxiv https://www.biorxiv.org/content/10.1101/2021.09.29.462357v1.full.

Author contributions: L.K.S., D.D.P., and C.D. designed research; L.K.S., A.K., J.S., and K.F. performed research; L.K.S., A.K., J.S., and K.F. analyzed data; and L.K.S., D.D.P., and C.D. wrote the paper.

Competing interest statement: D.D.P. is a founder, consultant, and shareholder of Hookipa Pharma, Inc., commercializing arenavirus-based vector technology, and is listed as an inventor on corresponding patents.

1. A. Harms, C. Dehio, Intruders below the radar: Molecular pathogenesis of *Bartonella* spp. *Clin. Microbiol. Rev.* **25**, 42–78 (2012).
2. A. Wagner, C. Dehio, Role of distinct type-IV-secretion systems and secreted effector sets in host adaptation by pathogenic *Bartonella* species. *Cell. Microbiol.* **21**, e13004 (2019).
3. M. A. Cheslock, M. E. Embers, Human bartonellosis: An underappreciated public health problem? *Trop. Med. Infect. Dis.* **4**, 69 (2019).
4. P. K. Mada, H. Zulfiqar, A. S. Joel Chandranesan, "Bartonellosis" in *StatPearls* (StatPearls Publishing, 2022). https://www.ncbi.nlm.nih.gov/books/NBK430874/?report=reader#_NBK430874_pubdet. Accessed 1 February 2022.
5. S. M. Akram, M. Y. Anwar, K. C. Thandra, P. Rawla, "Bacillary angiomatosis" in *StatPearls* (StatPearls Publishing, 2022). https://www.ncbi.nlm.nih.gov/books/NBK448092/. Accessed 1 February 2022.
6. C. Maguiña, H. Guerra, P. Ventosilla, Bartonellosis. *Clin. Dermatol.* **27**, 271–280 (2009).
7. M. J. Allison, A. Pezzia, E. Gerszten, D. Mendoza, A case of Carrion's disease associated with human sacrifice from the Huari culture of southern Peru. *Am. J. Phys. Anthropol.* **41**, 295–300 (1974).
8. M. F. Minnick *et al.*, Oroya fever and verruga peruana: Bartonelloses unique to South America. *PLoS Negl. Trop. Dis.* **8**, e2919 (2014).
9. A. Seubert, R. Schulein, C. Dehio, Bacterial persistence within erythrocytes: A unique pathogenic strategy of *Bartonella* spp. *Int. J. Med. Microbiol.* **291**, 555–560 (2002).
10. B. B. Chomel *et al.*, Ecological fitness and strategies of adaptation of *Bartonella* species to their hosts and vectors. *Vet. Res.* **40**, 29 (2009).
11. M. F. Minnick, J. M. Battisti, Pestilence, persistence and pathogenicity: Infection strategies of *Bartonella*. *Future Microbiol.* **4**, 743–758 (2009).
12. J. Koesling, T. Aebischer, C. Falch, R. Schülein, C. Dehio, Cutting edge: Antibody-mediated cessation of hemotropic infection by the intraerythrocytic mouse pathogen *Bartonella grahamii*. *J. Immunol.* **167**, 11–14 (2001).
13. G. Marignac *et al.*, Murine model for *Bartonella birtlesii* infection: New aspects. *Comp. Immunol. Microbiol. Infect. Dis.* **33**, 95–107 (2010).
14. K. L. Karem, Immune aspects of *Bartonella*. *Crit. Rev. Microbiol.* **26**, 133–145 (2000).
15. R. Schülein *et al.*, Invasion and persistent intracellular colonization of erythrocytes. A unique parasitic strategy of the emerging pathogen *Bartonella*. *J. Exp. Med.* **193**, 1077–1086 (2001).
16. D. C. Scherer, I. DeBuron-Connors, M. F. Minnick, Characterization of *Bartonella bacilliformis* flagella and effect of antiflagellin antibodies on invasion of human erythrocytes. *Infect. Immun.* **61**, 4962–4971 (1993).
17. H. Deng *et al.*, Identification and functional analysis of invasion associated locus B (IalB) in *Bartonella* species. *Microb. Pathog.* **98**, 171–177 (2016).
18. D. R. Burton, Antibodies, viruses and vaccines. *Nat. Rev. Immunol.* **2**, 706–713 (2002).
19. M. B. Oleksiewicz, G. Nagy, E. Nagy, Anti-bacterial monoclonal antibodies: Back to the future? *Arch. Biochem. Biophys.* **526**, 124–131 (2012).
20. A. E. Hall *et al.*, Characterization of a protective monoclonal antibody recognizing *Staphylococcus aureus* MSCRAMM protein clumping factor A. *Infect. Immun.* **71**, 6864–6870 (2003).
21. A. G. Barbour, V. Bundoc, In vitro and in vivo neutralization of the relapsing fever agent *Borrelia hermsii* with serotype-specific immunoglobulin M antibodies. *Infect. Immun.* **69**, 1009–1015 (2001).
22. H. Su, N. G. Watkins, Y. X. Zhang, H. D. Caldwell, *Chlamydia trachomatis*-host cell interactions: Role of the chlamydial major outer membrane protein as an adhesin. *Infect. Immun.* **58**, 1017–1025 (1990).
23. F. D. Menozzi *et al.*, Identification of a heparin-binding hemagglutinin present in mycobacteria. *J. Exp. Med.* **184**, 993–1001 (1996).
24. A. Watson *et al.*, Human antibodies targeting a *Mycobacterium* transporter protein mediate protection against tuberculosis. *Nat. Commun.* **12**, 602 (2021).
25. A. Harms *et al.*, Evolutionary dynamics of pathoadaptation revealed by three independent acquisitions of the VirB/D4 type IV secretion system in *Bartonella*. *Genome Biol. Evol.* **9**, 761–776 (2017).
26. R. Okujava *et al.*, A translocated effector required for *Bartonella* dissemination from derma to blood safeguards migratory host cells from damage by co-translocated effectors. *PLoS Pathog.* **10**, e1004187 (2014).
27. M. Vayssier-Taussat *et al.*, The Trw type IV secretion system of *Bartonella* mediates host-specific adhesion to erythrocytes. *PLoS Pathog.* **6**, e1000946 (2010).
28. A. Bergthaler *et al.*, Impaired antibody response causes persistence of prototypic T cell-contained virus. *PLoS Biol.* **7**, e1000080 (2009).
29. J. K. Whitmire, M. K. Slifka, I. S. Grewal, R. A. Flavell, R. Ahmed, CD40 ligand-deficient mice generate a normal primary cytotoxic T-lymphocyte response but a defective humoral response to a viral infection. *J. Virol.* **70**, 8375–8381 (1996).
30. M. F. Bachmann, L. Hunziker, R. M. Zinkernagel, T. Storni, M. Kopf, Maintenance of memory CTL responses by T helper cells and CD40-CD40 ligand: Antibodies provide the key. *Eur. J. Immunol.* **34**, 317–326 (2004).
31. C. M. Litwin, J. M. Johnson, Identification, cloning, and expression of the CAMP-like factor autotransporter gene (cfa) of *Bartonella henselae*. *Infect. Immun.* **73**, 4205–4213 (2005).
32. J. R. H. Tame, Autotransporter protein secretion. *Biomol. Concepts* **2**, 525–536 (2011).
33. H. L. Saenz *et al.*, Genomic analysis of *Bartonella* identifies type IV secretion systems as host adaptability factors. *Nat. Genet.* **39**, 1469–1476 (2007).
34. J. A. Capra, M. Singh, Predicting functionally important residues from sequence conservation. *Bioinformatics* **23**, 1875–1882 (2007).
35. J. Jumper *et al.*, Highly accurate protein structure prediction with AlphaFold. *Nature* **596**, 583–589 (2021).
36. M. Rojas-Lopez *et al.*, Identification of the autochaperone domain in the type Va secretion system (T5aSS): Prevalent feature of autotransporters with a β-helical passenger. *Front. Microbiol.* **8**, 2607 (2018).

37. M. Québatte *et al.*, Gene transfer agent promotes evolvability within the fittest subpopulation of a bacterial pathogen. *Cell Syst.* **4**, 611–621.e6 (2017).
38. M. Québatte, C. Dehio, *Bartonella* gene transfer agent: Evolution, function, and proposed role in host adaptation. *Cell. Microbiol.* **21**, e13068 (2019).
39. M. J. Gardner *et al.*, Genome sequence of the human malaria parasite *Plasmodium falciparum*. *Nature* **419**, 498–511 (2002).
40. X. Z. Su *et al.*, The large diverse gene family var encodes proteins involved in cytoadherence and antigenic variation of *Plasmodium falciparum*-infected erythrocytes. *Cell* **82**, 89–100 (1995).
41. D. B.-C. Wu, N. Chaiyakunapruk, H.-Y. Chong, P. Beutels, Choosing between 7-, 10- and 13-valent pneumococcal conjugate vaccines in childhood: A review of economic evaluations (2006–2014). *Vaccine* **33**, 1633–1658 (2015).
42. T. F. Meyer, J. P. van Putten, Genetic mechanisms and biological implications of phase variation in pathogenic neisseriae. *Clin. Microbiol. Rev.* **2** (suppl.), S139–S145 (1989).
43. N. Lewis-Rogers, J. Seger, F. R. Adler, Human rhinovirus diversity and evolution: How strange the change from major to minor. *J. Virol.* **91**, e01659-16 (2017).
44. B. E. Correia *et al.*, Proof of principle for epitope-focused vaccine design. *Nature* **507**, 201–206 (2014).
45. I. Sorg *et al.*, A *Bartonella* effector acts as signaling hub for intrinsic STAT3 activation to trigger anti-inflammatory responses. *Cell Host Microbe* **27**, 476–485.e7 (2020).
46. Y. Perez-Riverol *et al.*, The PRIDE database and related tools and resources in 2019: Improving support for quantification data. *Nucleic Acids Res.* **47**, D442–D450 (2019).